An Experimental and Analytical Study in Reinforced Concrete Frames with Weak Beam-Column Joints

B. Bayhan
Mersin University, Mersin, Turkey

J.P. Moehle
University of California, Berkeley

S. Yavari & K.J. Elwood
University of British Columbia, Vancouver

S.H. Lin, C.L. Wu & S.J. Hwang
National Center for Research on Earthquake Engineering, Taipei

SUMMARY:
This paper describes an experimental and analytical study in reinforced concrete frames with weak beam-column joints. A 1/2.25 scale, planar, two-story by two-bay reinforced concrete frame was subjected to earthquake simulations on the shaking table. The beam-column connection did not contain transverse reinforcement that is typical in older-type construction. To our knowledge, no shaking table tests on frames failing in unreinforced beam-column joints have been reported. Linear and nonlinear analytical models based on the modeling procedures of ASCE/SEI 41 Supplement 1 were carried out and subjected to the input base motions. Our results illustrate that the calculated response does not provide reasonably accurate values for the measured one.

Keywords: Reinforced concrete, weak beam-column joints, shaking table, analytical model, ASCE/SEI 41 Sup.1

1. GENERAL INSTRUCTIONS

Design procedures for earthquake-resistant reinforced concrete frames, based on ductile behavior of the system were introduced in the 1960s (Blume et al., 1961) and have been adapted to modern building practices worldwide (e.g., ACI 318, 2011; AIJ 1994; NZS 3101, 2006). Buildings constructed prior to the adoption of these modern practices may contain deficiencies that make them especially vulnerable to damage or collapse during earthquake shaking. Procedures for seismic assessment (ASCE/SEI 31 2003) and rehabilitation (ASCE/SEI 41 Sup.1 2008) of existing buildings have been developed but have not been widely tested against actual response of older-type construction subjected to earthquake base motions.

In this study we examine the seismic response of a deficient reinforced concrete frame, tested on the shaking table, and the accuracy of various procedures for analytically assessing its global response. The test structure was a reduced-scale, planar, two-story by two-bay reinforced concrete frame constructed with ductile columns and without transverse reinforcement in the beam-column joints (Yavari 2011). The frame was subjected to earthquake simulations, resulting in severe damage to the beam-column joints. Linear and nonlinear analytical models consistent with the modeling procedures of ASCE/SEI 41 Supplement 1 (2008) were subjected to the input base motions. The results provide a basis for judging the accuracy of various modeling assumptions and demonstrate the importance of modeling beam-column joint nonlinearity for the case of buildings with deficient joints.

2. SHAKING TABLE TESTS

2.1. Test Structure

The test structure studied here was part of a series of test structures investigating seismic behavior of older-type reinforced concrete frames (Yavari 2011). The specimen was a 1/2.25-scale, two-story by two-bay reinforced concrete frame tested on the shaking table at the National Center for Research on

Earthquake Engineering (NCREE) in Taiwan. Member dimensions were selected to be representative of those in a six-story building. Final dimensions and reinforcement details of the frames were influenced by the laboratory limitations, desired failure mode, and cost. The target failure mode was intended to occur in the beam-column joints of the lower story. Figure 1 shows the geometry and reinforcement of the test structure.

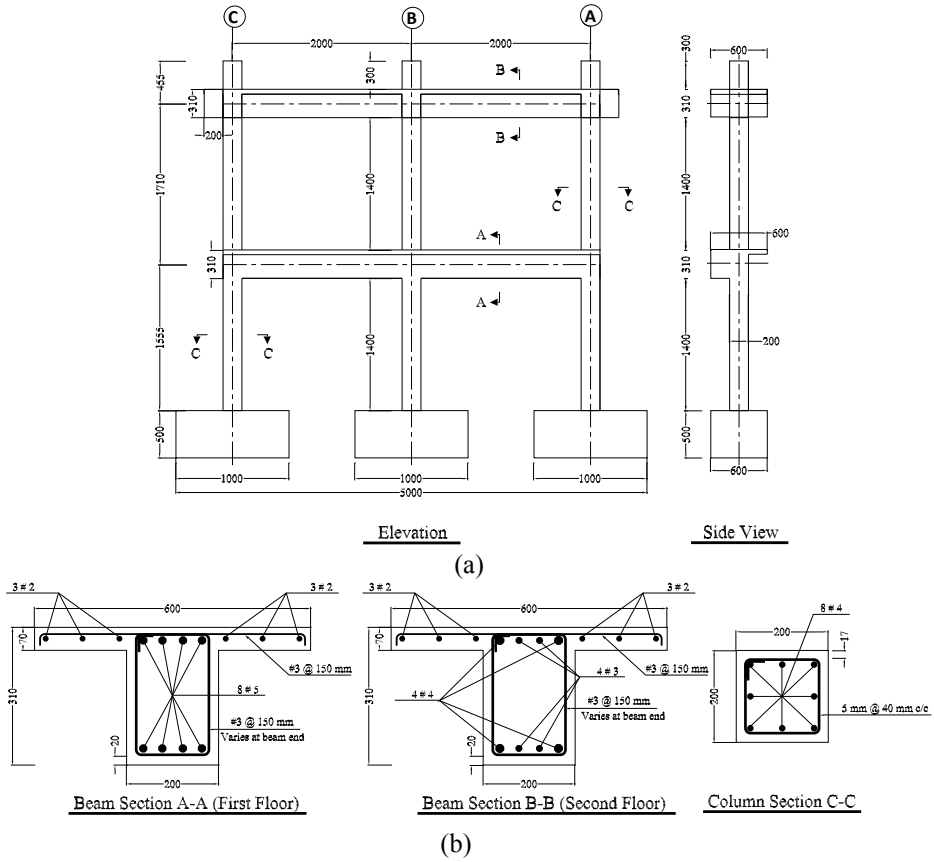

Figure 1. (a) Shaking table test specimen and (b) reinforcement details. Units are mm (Yavari 2011)

Lower-story columns frame into supporting footings with moment-resisting connections. For reference in this paper, the base corresponds to the top of the footings. Levels 1 and 2 refer to the first and second elevated beams. Columns are identified by their axis letter (Figure 1) and story number; thus, Column A1 is the first-story column at axis A. Joints have similar nomenclature, with the number indicating the level; thus, Joint A1 is the joint immediately above Column A1.

Beam-column joints at Level 1 did not have transverse reinforcement. As shown in Figure 1a, transverse beam stub was cast on one side of the beam-column joints at this level to simulate confinement from transverse beams on one side as would be typical of an exterior frame. Beam-column joint failure was not desirable at Level 2 because frame boundary conditions were not well simulated. To strengthen the joints at Level 2, joints were reinforced with transverse reinforcement and beam stubs were provided at both sides of the joints.

Beams and columns of the test frame were designed so that inelastic response, if it occurred in those components, would be in a ductile flexural mode without shear or splice failure. Beam longitudinal reinforcement was chosen to create a weak-column-strong-beam mechanism, not unusual in older concrete construction. Columns were reinforced with continuous longitudinal bars (without splices), resulting in total longitudinal reinforcement ratio of 0.026. It was desirable to have widely spaced column transverse reinforcement so as to not interfere with joint failure mechanisms (which tend to spread into the column), while also ensuring that column shear failure would not occur. The provided transverse reinforcement ratio for all columns was 0.0049 (ρ" = A_{st}/bs where A_{st} is the area of transverse reinforcement parallel to the plane of the frame with spacing s, and b is the column width),

with a spacing of 0.2b. Using ASCE/SEI 41 Supplement 1 (2008), the ratio of the plastic shear demand (V_p) to the nominal shear strength (V_n) for the columns was 0.41, indicating that the columns would be governed by flexural yielding.

The frame was designed so that the sum of beam flexural strengths exceeded the sum of column flexural strengths at each joint. Therefore, Level 1 joint demands can be estimated based on the beam flexural tension and compression forces required to equilibrate the joint when the columns develop nominal flexural strengths above and below a joint (ACI 352 2002). Joint nominal strengths, based on ASCE/SEI 41 Supplement 1 (2008), are

$$V_n = 0.083\gamma\sqrt{f_c'}A_j \text{ (MPa)} \tag{1}$$

where A_j is the joint area and γ is a coefficient depending on joint geometry. For exterior joints with and without transverse beams γ =8 and 6, respectively, whereas for interior joints with and without transverse beams γ =12 and 10, respectively. Because only one transverse beam frames into the joint, interpolated values of γ =7 and 11 are adopted for exterior and interior joints of the test frame, respectively. Using these procedures, ratios of joint demands to joint nominal strengths are 2.4 and 1.8 at exterior and interior joints.

2.2. Test Setup

The specimen was bolted atop six load cells (two per column), which were previously bolted to the shaking table (Figure 2). A stiff steel frame (not shown) sandwiched the concrete test frame; a low-friction roller system connecting between the steel and concrete frames provided out-of-plane stability at each level while permitting essentially free in-plane motion (both horizontal and vertical) of the concrete test frame.

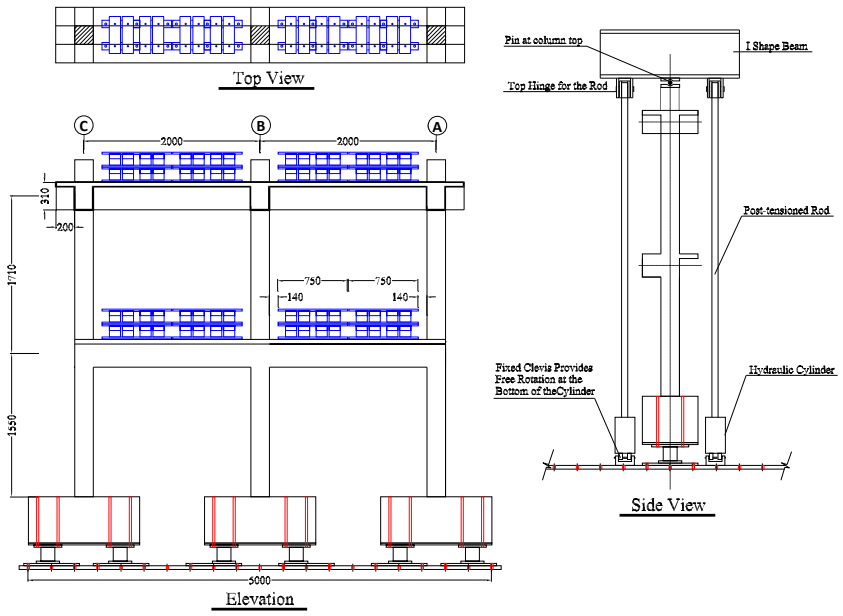

Figure 2. Test setup showing subsidiary mass, post-tensioning, and load cells (Yavari 2011)

Subsidiary mass (lead plus steel) was attached to the top surfaces of the beams to simulate tributary gravity and inertial loads at those levels (19.6 kN at Level 1 and 18.9 kN at Level 2). Because the test frame was intended to represent the lower two stories of a six-story building, additional measures were necessary to partially simulate effects of the upper stories. Horizontal inertial mass was simulated by placing 104 kN of additional mass in roller-supported carts rigidly linked to the Level 2 beams. In addition, external post-tensioning applied additional axial loads through pin connections at the top of

the columns. The post-tensioning plus gravity loads achieved column axial loads at the base of the frame equal to $0.2f'_cA_g$ for Column B1 and $0.1f'_cA_g$ for Columns A1 and C1. A pressure-regulating valve kept the applied axial load approximately constant during the tests. Note that this method of axial load application does not correctly account for P-delta effects. Higher-mode effects associated with a complete 6-story building model are also not simulated.

2.3. Input Base Motions

The north-south (NS) component of the TCU047 accelerogram from the 1999 Chi-Chi Taiwan earthquake (M_w=7.6) was used as the input motion. Station TCU047 (24.6188° N latitude, 120.9387° longitude) was 33 km from the surface rupture and recorded a peak ground acceleration (PGA) of 0.41 g in the NS direction. The ground motion was time-scaled by the square root of 1/2.25 (in consideration of similitude laws for reduced-scale specimens) and amplitude-scaled to different amplitudes for different tests. In four shaking table tests the peak table accelerations were recorded as 0.25g, 0.84g, 1.11g, and 1.36g. The measured table motion for the 0.84g test and the elastic response spectra for 3% damping for each test are shown in Figure 3.

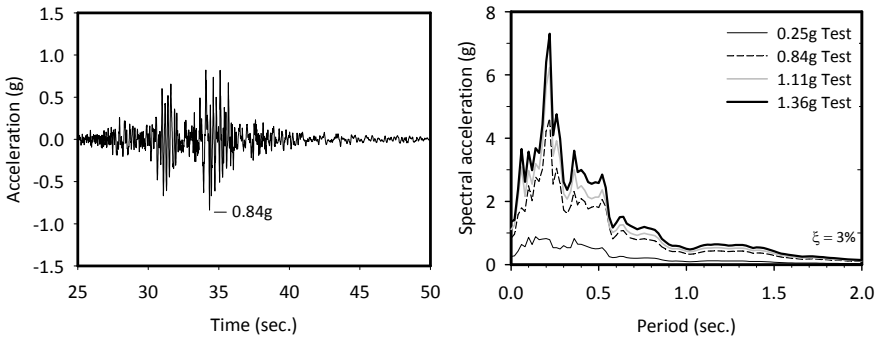

(a) (b)

Figure 3. (a) Base acceleration history recorded on the shaking table for the 0.84g Test and (b) Linear response spectra (3% damping) for the four base motions recorded on the shaking table

2.4. Observed Response

Dynamic response of the test structure and its resulting damage were recorded for each of the four sequential earthquake simulations. Figure 4 shows typical results obtained during the second test for which peak base acceleration reached 0.84g.

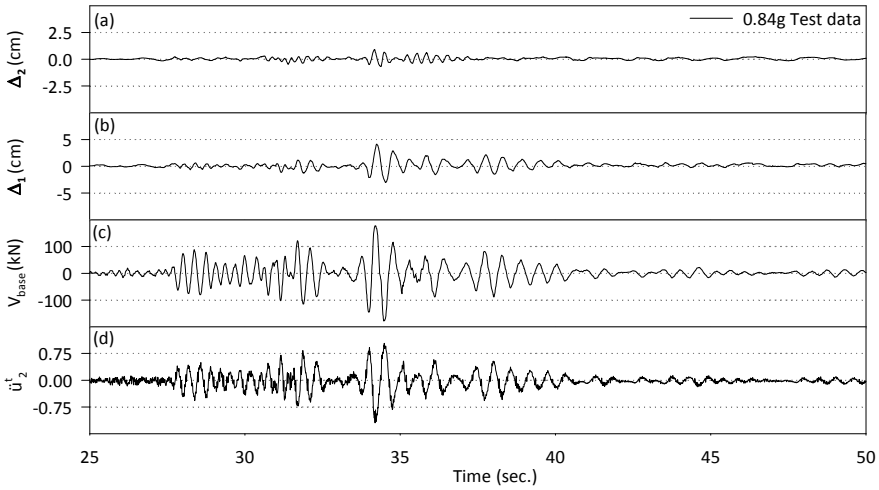

Figure 4. Measured response histories for the 0.84g test (a) 2nd level displacement, (b) 1st level displacement, (c) base shear, and (d) 2nd level acceleration, ($\ddot{u}_2^t$: second level acceleration)

The dynamic response was dominated by an apparent first mode, which might be expected considering the large mass concentrated at Level 2 in the test setup. Based on white noise tests conducted before the test, the period of vibration was approximately 0.29 s at the beginning of the test. The effective period had elongated to approximately 0.46 s at the end of the test, suggesting that the effective flexibility of the structure had increased by a factor of $(0.46/0.29)^2 = 2.5$.

Figure 5 plots relations among peak displacements, peak base shears, and peak base accelerations measured for each of the four earthquake simulations. Peak Level 2 displacement (relative to the base) increased approximately linearly with increasing peak base acceleration (Figure 5a). In contrast, the relation between peak base shear and peak displacement is highly nonlinear and suggests that the structure had reached its apparent base-shear strength during 0.84g test and was degrading in strength with subsequent shaking (Figure 5b).

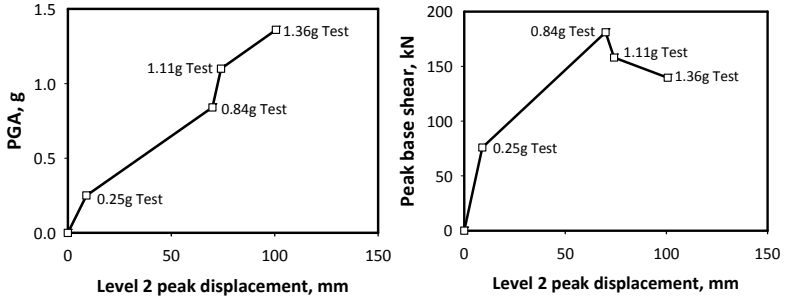

(a) (b)

Figure 5. Relation between (a) Level 2 peak base acceleration and peak displacement, and between (b) peak base shear and Level 2 peak displacement. Peak quantities are the maximum absolute values of the respective quantities recorded during a test.

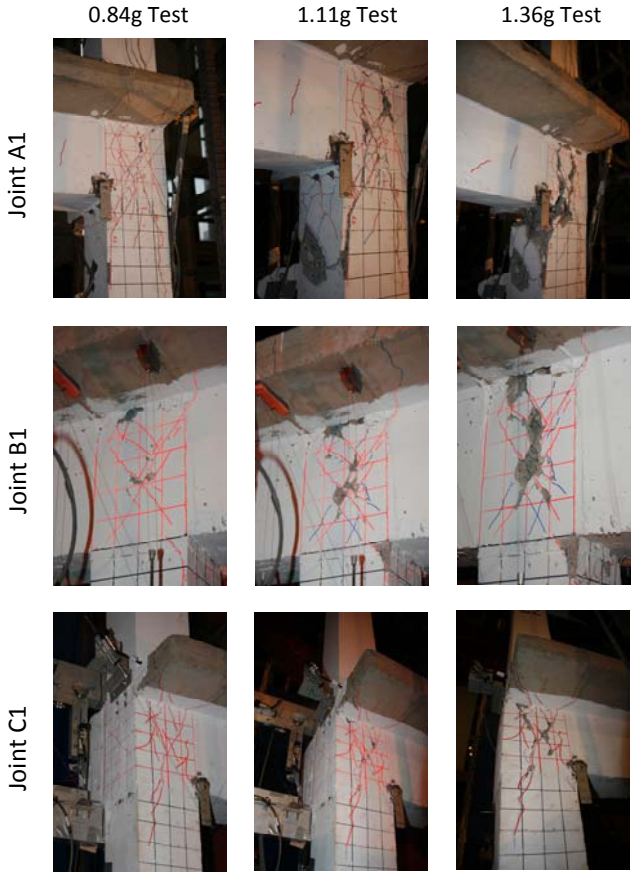

Figure 6. Photographs of damage for joints A1, B1, and C1 for the (a) 0.84g, (b) 1.11g, and (c) 1.36g Tests

The test structure was examined visually following each earthquake simulation. No cracks were observed following the 0.25g test. In the 0.84 g test, flexural cracks developed at the bottom of first-story columns and diagonal cracks developed in the Level 1 joints (Figure 6a). During the 1.11 g test, the extent of flexural cracking in the first-story columns increased, the cover concrete at the bottom of column B1 partially spalled, and minor flexural cracking occurred at the top of column B2. In the final test (1.36g test), inclined cracking in joints B1 and C1 increased and joint A1 sustained severe damage (Figure 6c).

3. ANALYTICAL MODELS OF THE SIMULATION

Two analytical models were developed without considering the shaking table test results in order to provide a "blind" comparison of the measured and analytical results and to objectively evaluate the accuracy of existing procedures. The first model follows the linear modeling recommendations of ASCE/SEI 41 Supplement 1 (2008), the second model introduces nonlinear column elements with bar slip springs to represent column behavior. The sequence of table motions was considered to be similar to the experiment and residual damages were accumulated from the sequential tests. The average compressive strength of concrete cylinders was measured as 35.8 MPa. The yield strength of the longitudinal reinforcement was 467 MPa from the rebar coupon tests. Since the white noise test data suggests a damping value close to 3%, Rayleigh damping is introduced to the all models through mass and stiffness-proportional coefficients resulting in 3% damping ratio for the first and second modes. Fluctuation in external post-tensioning applied additional axial loads at the top of the columns was considered in the analyses of analytical models.

3.1. Model 1-Linearly Elastic Model

The first analytical model (Model 1) implements the linear modeling recommendations of ASCE/SEI 41 Supplement 1 (2008) using the software platform OpenSees (2005). The model (Figure 7) consists of line elements with linear-elastic properties, with reduced effective flexural stiffness accounting for the slip of reinforcement from anchorages. The effective stiffness of the exterior columns with low axial load ($P/A_g f_c' = 0.1$) and that of interior columns with moderate axial load ($P/A_g f_c' = 0.2$) is taken as $0.3EI_g$ and $0.4EI_g$, respectively, where E is concrete modulus of elasticity and I_g is the gross section moment of inertia. The beams have reduced effective stiffness value of $0.3EI_g$. Effects of joint shear deformations are approximated by extending the column flexibility into the joint (as recommended in ASCE/SEI 41 Supplement 1 2008) wherever $\Sigma M_{nc}/\Sigma M_{nb} < 0.8$, where ΣM_{nc} and ΣM_{nb} are the sum of the nominal moment strengths of the columns and beams, respectively, at a beam-column connection). Beam elements are taken as rigid within the dimensions of the joint. The footings are assumed to be linear elastic members due to their relatively large size, and supporting load cells also are modeled, though their flexibility is found to be negligible. The weight of the beam and lead weights are considered as point loads and lumped masses at the beam nodes.

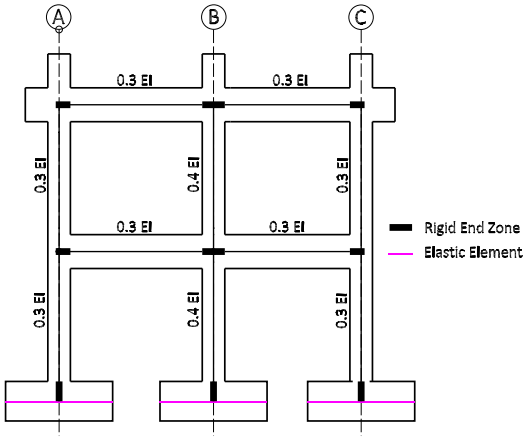

Figure 7. Model 1 implements the linear modeling recommendations of ASCE/SEI 41 Sup. 1 (2008)

The fundamental period of vibration of Model 1 was calculated as 0.36 s, which is longer than the initial period of 0.29 s (estimated from a white noise test after the first earthquake simulation test). The longer calculated period is expected, because the structure responded well below the yield point at this stage of testing whereas the ASCE/SEI 41 Sup. 1 (2008) modeling procedures are intended to model response near the yield point. During subsequent earthquake simulations, the calculated period was shorter than the ever elongating apparent periods achieved during those tests. Because the vibration period of the analytical model did not match the apparent periods in any of the tests, it is not surprising that the calculated displacement waveforms mismatched all the measured displacement waveforms (Figure 10).

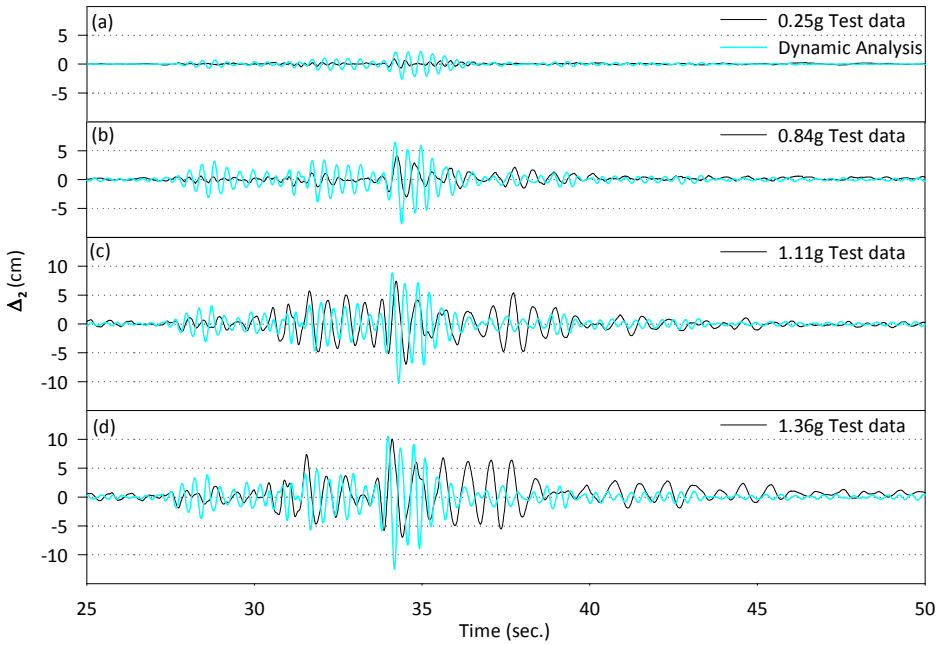

Figure 6. Measured and calculated (Model 1) relative displacement response histories for Level 2 measured during the (a) 0.25g, (b) 0.84g, (c) 1.11g, and (d) 1.36g Tests.

As expected, base shears shown in Table 1 were over-estimated for all tests, particularly for the second, third, and fourth tests, because the analytical model assumed linear behavior whereas for those tests the base shear was limited by nonlinear response.

Table 3.1. Measured and calculated peak 2nd level displacement (Δ_2), 1st level displacement (Δ_1), base shear (V_b) and total acceleration ($\ddot{u}_2 + \ddot{u}_{base}$) for all models (M1:Model 1, M2:Model 2) and earthquake simulations. PBA(g): Peak Base(shaking table) Acceleration. *Errors (%) are shown below the calculated values in italics.*

Measured					**Calculated**							
PBA	**Δ_2**	**Δ_1**	**V_b**	**$\ddot{u}_2+\ddot{u}_b$**	**Δ_2 (mm)**		**Δ_1 (mm)**		**V_b (kN)**		**$\ddot{u}_2+\ddot{u}_b$ (g)**	
(g)	**(mm)**	**(mm)**	**(kN)**	**(g)**	**M1**	**M2**	**M1**	**M2**	**M1**	**M2**	**M1**	**M2**
0.25	9	7	75.3	0.46	26	10	11	5	112	79	0.81	0.50
					186	*13*	*69*	*20*	*48*	*5*	*77*	*9*
0.84	70	42	181	1.2	77	42	33	23	330	216	2.34	1.39
					9	*40*	*21*	*44*	*82*	*19*	*95*	*16*
1.11	74	42	158	1.07	103	64	44	40	446	237	3.11	1.60
					38	*13*	*6*	*3*	*182*	*50*	*191*	*50*
1.36	101	57	140	1.03	125	115	54	81	538	262	3.76	1.75
					24	*15*	*6*	*43*	*285*	*88*	*263*	*69*

3.2. Model 2-Nonlinear Column Model

An apparent shortcoming in Model 1 is that all components were modeled as being linear-elastic whereas the test structure responded inelastically. As a first step in modeling inelastic response, Model 2 introduces nonlinear elements for the columns, including linear springs to represent rigid body rotations associated with reinforcement slip from anchorages. Beams were designed to respond in the effectively linear range of response, so they were modeled using linear elements with effective stiffness ($0.3EI_g$ as in Model 1). Joints were assumed rigid. Rayleigh damping was introduced using the same approach as used for Model 1. Figure 7 illustrates the geometry of the analytical model.

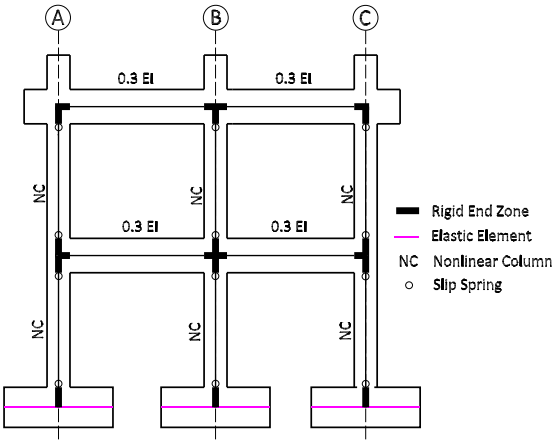

Figure 7. Model 2 implements linear beam elements, nonlinear column elements, and linear slip springs at both ends of columns

Column flexure was represented by force-based, fiber nonlinear beam-column elements with five integration points. The formulation of these elements assumes that plane sections remain plane and normal to the longitudinal axis at each integration point. Spread of plasticity is modeled using the Gauss-Lobatto quadrature rule through the element (Spacone et al. 1996). Column shear deformations are ignored. Unconfined and confined concrete is modeled using the stress-strain model of Mander et al. (1998). The confined concrete material strength was calculated as 43.5 MPa. The longitudinal reinforcement was modeled using the OpenSees hysteretic material model (OpenSees 2005).

Zero length linear-elastic section elements are added to both ends of columns to simulate rotations due to slip of reinforcement from adjacent anchorages. The rotational stiffness of the slip springs, k_{slip}, is calculated by assuming a constant bond stress of u=0.8 MPa along the column longitudinal bars within the footings and the beam-column joints until the calculated stress drops to zero, estimating bar slip as the total elongation of the bar along this stressed anchorage length, and assuming section rotation occurs about the cracked section neutral axis. With these assumptions, the rotational spring stiffness is (Elwood and Eberhard 2009)

$$k_{slip} = \frac{8u}{d_b f_y} \frac{M_{0.004}}{\phi_y} = \frac{8u}{d_b f_y} EI_{flex} \qquad (1)$$

where d_b is the nominal diameter of the longitudinal reinforcement, f_y is the longitudinal reinforcement yield stress, $M_{0.004}$ is the calculated moment strength corresponding to strain 0.004 in the extreme compression fiber of concrete, ϕy is the yield curvature for the cracked section, and EI_{flex} is effective flexural rigidity of the cracked section.

The fundamental period of vibration of Model 2 (0.28 s) is shorter than that of Model 1 (0.36 s), and very close to the initial period of 0.29 s measured in white noise tests. The calculated response for the 0.25g and 0.84g test is relatively well synchronized with the measured response (Figures 8a and 8b).

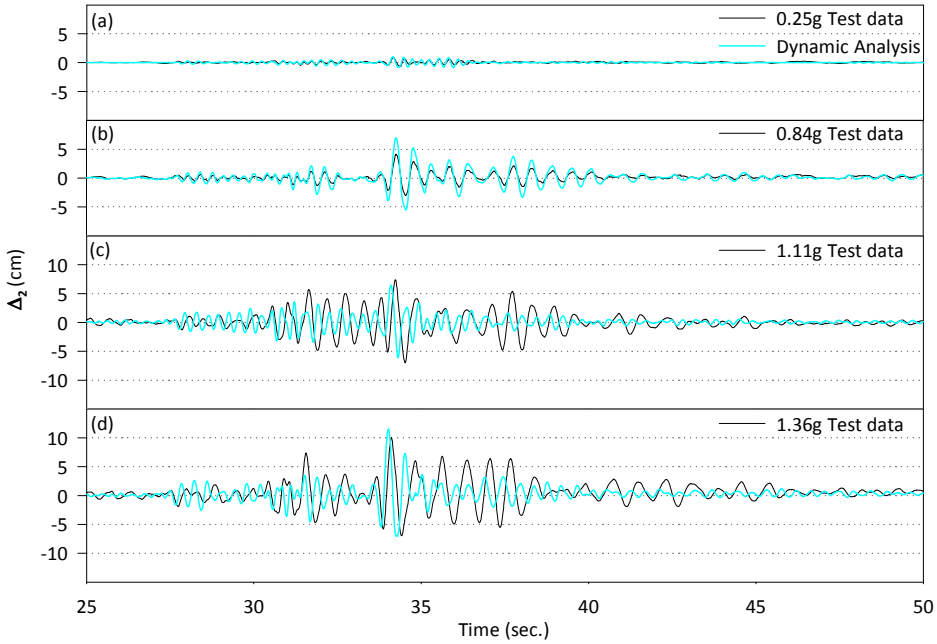

Figure 8. Measured and calculated (Model 2) relative displacement response histories for Level 2 measured during (a) 0.25 g, (b) 0.84 g, (c) 1.11 g, and (d) 1.36 g tests

For subsequent earthquake simulation tests (1.11g and 1.36g tests) in which joint cracking increased, however, the apparent period of the analytical model with rigid joints is shorter than the apparent period of the test structure, such that calculated and measured waveforms are poorly synchronized (Figures 8c and 8d). As summarized in Table 3.1, estimates of peak displacement are inconsistent especially for the 0.84g test. The calculated errors are 40% and 44% for Level 2 and Level 1 displacements, respectively. Peak base shears were poorly estimated except for the 0.25g and 0.84g earthquake simulations. The calculated values exceeded the measured values by a considerable margin particularly for the 1.11g and 1.36g tests.

4. CONCLUSION

A 1/2.25 scale, planar, two-bay by two-story reinforced concrete frame without transverse reinforcement in the first-level beam-column joints was subjected to subsequent earthquake simulations on a shaking table. The joints sustained considerable damage indicating occurrence of inelastic joint response during the tests. Linear and nonlinear analytical models of the test structure were developed based on the recommendations of ASCE/SEI 41 Supplement 1 (2008). The analytical models and their analyses were based on measured geometries, material properties, and input base motions, but otherwise the analyses were intended as "blind analyses" in the sense that "tuning" of model parameters to improve correlation was not pursued. Within the limitations of these tests and analyses, the following conclusions are made:

1. The fundamental period of the linear model incorporating the stiffness modeling recommendations of ASCE/SEI Sup. 1 (2008) had longer period than the effective period measured during 0.25g test. Since the test structure responded essentially elastically (well below the yield point) for this test and the ASCE/SEI Sup.1 (2008) modeling procedures are intended to model response near the yield point, a longer calculated period was expected. However, the calculated period was shorter than the apparent period during subsequent tests. Consequently, the analytical simulation using Model 1 did not match well with the measured simulations for any of the tests.
2. The addition of nonlinear column models to the analytical model improved the correlation with all tests, but the model (Model 2) was still too stiff and strong for second to fourth tests. As a result, the analytical models ignoring the effects of joint nonlinearity in deficient joints could not produce accurate correlation with the test results.

AKCNOWLEDGEMENT

This study was funded by the U.S. National Science Foundation as part of the NEES Grand Challenge Project on Mitigation of Collapse Risk in Vulnerable Concrete Buildings, under Award No. 0618804 to the Pacific Earthquake Engineering Research Center, University of California, Berkeley. The laboratory tests were funded in part by the National Science Council of Taiwan under Award No. NSC94-2625-Z-492-005. The funding, facilities, and technical support from the National Center for Research on Earthquake Engineering of Taiwan are gratefully acknowledged. All opinions expressed are solely those of the authors and do not necessarily represent the views of the funding agencies.

REFERENCES

American Concrete Institute (2002). Recommendations for Design of Beam-Column Connections in Monolithic Reinforced Concrete Structures, ACI 352-02, Farmington Hills, Michigan.

American Concrete Institute (2011). Building Code Requirements for Structural Concrete and Commentary, ACI 318-11, Farmington Hills, Michigan.

American Society of Civil Engineers (2003). Seismic Evaluation of Existing Buildings, ASCE/SEI 31-03, Reston, Virginia.

American Society of Civil Engineers (2008). Seismic Rehabilitation of Existing Buildings, ASCE/SEI41 Supplement 1, Reston, Virginia.

Architectural Institute of Japan (1994). AIJ Structural Design Guidelines for Reinforced Concrete Buildings (English Translation), Tokyo.

Blume J. A., Newmark N. M. and Corning L. H. (1961). Design of Multistory Reinforced Concrete Buildings for Earthquake Motions, Portland Cement Association, Chicago.

Elwood K. J., and Eberhard M. O., 2009. Effective stiffness of reinforced concrete columns. *ACI Structural Journal* **106:4**, 476-484.

Mander J. B., Priestley M. J. N. and Park R., (1988). Theoretical stress–strain model for confined concrete, *Journal of Structural Engineering* **114:8**, 1804–1826.

OpenSees (2005). Open System for Earthquake Engineering Simulation, Pacific Earthquake Engineering Research Center, University of California, Berkeley.Available from:http://www.opensees.berkeley.edu

Spacone E., Filippou F. C. and Taucer F. F. (1996). Fiber beam–column model for non-linear analysis of R/C frames. Part I: Formulation and Part II: Application, *Earthquake Engineering and Structural Dynamics* **25:7**, 711–742.

Standards Association of New Zealand (2006). Concrete Design Standard, NZS3101:2006, Part 1 and Commentary on the Concrete Design Standard, NZS 3101:2006, Part 2. Standards Association of New Zealand, Wellington.

Yavari S. (2011). Shaking Table Tests on the Response of Reinforced Concrete Frames with Non-Seismic Detailing, Ph.D. Dissertation, Department of Civil Engineering, University of British Columbia, 2011.